Deep Reinforcement Learning for Orienteering Problems Based on Decomposition

Wei Liu, Tao Zhang, Rui Wang, Kaiwen Li, Wenhua Li, and Kang Yang

***Abstract*—This paper presents a new method for solving an orienteering problem (OP) by breaking it down into two parts: a knapsack problem (KP) and a traveling salesman problem (TSP). A KP solver is responsible for picking nodes, while a TSP solver is responsible for designing the proper path and assisting the KP solver in judging constraint violations. To address constraints, we propose a dual-population coevolutionary algorithm (DPCA) as the KP solver, which simultaneously maintains both feasible and infeasible populations. A dynamic pointer network (DYPN) is introduced as the TSP solver, which takes city locations as inputs and immediately outputs a permutation of nodes. The model, which is trained by reinforcement learning, can capture both the structural and dynamic patterns of the given problem. The model can generalize to other instances with different scales and distributions. Experimental results show that the proposed algorithm can outperform conventional approaches in terms of training, inference, and generalization ability.**

***Index Terms*—Orienteering Problem, Decomposition, Evolutionary Algorithm, Deep Reinforcement Learning, Attention.**

I. Introduction

It is common for tourists to plan trip routes with limited durations and limited numbers of scenic stops. Tourists intend to visit series of spots that are located in different places and have different scores for quantifying tourists' levels of interest; a trip starts and ends at a specific location called the depot. Within the given tour time, the goal is to maximize the total score of the nodes visited in a single tour. This is an orienteering problem (OP) [1], which has applications not only in tourist trip design [2] but also in home fuel delivery [3] and unmanned aerial vehicle (UAV) reconnaissance mission planning, among other scenarios.

An OP can be defined by a complete graph $G = (V, A)$, where $V = \{v_1, \ldots, v_N\}$ is the vertex set and $A = (\{i, j\} : i, j \in N)$ is the arc set. A nonnegative real number s_i called the score associated with each vertex $v_i \in V$ and a positive real number t_{ij} called the travel time or travel distance associated with each arc $\{i, j\} \in A$ are present. The goal of the OP is to determine a Hamiltonian path over a subset of V (including the starting and ending vertices) to maximize the total score derived from the visited vertices, while the path length cannot exceed a given limitation T_{max}. By default, we set the starting and the ending vertices as the same point. The OP can then be formulated as a linear programming problem as described by [3]. It should be noted that the travel distance t_{ij} in this work is defined as the Euclidean distance between the vertices, which also means that $t_{ij} = t_{ji}$.

As nondeterministic polynomial (NP)-hard problems [1], OPs are some of the most classic combinatorial optimization problems, and they have been studied for decades. During the last decade, several exact and heuristic algorithms have been proposed to solve this type of problem as well as its variants. Exact algorithms, including the branch-and-bound [4], [5], cutting plane [6] and branch-and-cut algorithms [7], [8], have been applied to solve OPs. With exact algorithms, it is difficult to solve large-scale cases in limited time periods; in such cases, heuristics show their advantages. Iterative local search (ILS) [2] is one of the most famous heuristics aimed at the OP family; it can provide satisfactory solutions with good speed. Based on that, several local research options have been introduced to improve the ILS approach [9]. More recently, a large number of advanced heuristic algorithms, such as effective neighborhood search [10], large neighborhood search [11], variable neighborhood search, ant colony system [12], tabu search [13], and simulated annealing heuristics [14], [3], have been applied. Recently, to save on development costs and enhance model generalization, learning heuristics for combinatorial optimization problems have been the focus. In particular, deep reinforcement learning (DRL) methods have already been applied to solve OPs and their variants [15], [16] in the past three years. While many methods are already available for solving OPs, considering the complexity induced by time constraints and the variable lengths of solutions, the existing methods still have difficulty dealing with dynamic data in a quick and precise manner, especially for large-scale cases. Therefore, it is necessary to design a new method that inherits the advantages of the above algorithms, including the traditional heuristics and learning heuristics.

Essentially, an OP is a combination of node selection and shortest Hamiltonian path planning among the selected nodes [3], which means that an OP can be decomposed into two other classic combinatorial optimization problems: a knapsack problem (KP) and a traveling salesman problem (TSP). In detail, the KP solver aims at selecting nodes of interest to obtain the highest total score under the given constraints, and the TSP solver tries to generate a single path among the selected nodes with the minimum traveling time, which helps the KP solver judge the feasibility of its solutions and enables it to make further adjustments. Finally, OP solutions

This paper is partially supported by the National Natural Science Foundation of China (no. 72071205, no. 61873328 and no. 61773390).*(Corresponding authors: Tao Zhang; Rui Wang.)*

Wei Liu, Tao Zhang, Rui Wang, Kaiwen Li, Wenhua Li and Kang Yang are with the College of System Engineering, National University of Defense Technology, Changsha 410073, PR China, and with the Hunan Key Laboratory of Multi-Energy System Intelligent Interconnection Technology, HKL-MSI2T, Changsha 410073, PR China. (e-mail: weiliu16@nudt.edu.cn, zhangtao@nudt.edu.cn, ruiwangnudt@gmail.com, kaiwenli_nudt@foxmail.com, yangkang20@nudt.edu.cn)

can be obtained by iteratively adjusting the solutions of the KP. Considering that the advanced algorithms for solving KPs and TSPs are highly mature, it is reasonable to solve an OP by decomposing it into a KP and a TSP. However, to date, no study has applied this decomposition method (DM) in reality. Traditional methods for solving TSPs, whether they are exact algorithms or heuristic algorithms, are all specifically designed for particular instances, which means that they need complete the solving procedure once again if the problem changes even by only one data point. Since the DM requires solving the TSP on different occasions, repeatedly training TSP models is uneconomical.

Fortunately, machine learning algorithms with strong generalization abilities and fast solution speeds can solve this puzzle perfectly, and they currently perform satisfactorily in terms of solving various problems, including TSPs. Vinyals [17] introduced the concept of the pointer network (PN), which is a kind of neural network inspired by sequence-to-sequence models, to solve a TSP via supervised learning. Once the network is trained, it can immediately output the correct node access sequence (near-optimal TSP tour) based on the input node information. It has a great advantage in terms of evaluation time over traditional combinatorial optimization algorithms, which generally optimize solutions in an iterative manner. However, the supervised learning method requires a large number of existing solutions, which may be difficult to obtain for most problems. At the same time, these provided solutions greatly limit the quality of the solution found by the PN.

Without the requirements of existing solutions, reinforcement learning (RL) can optimize policies via autonomous learning. Bello et al. [18] presented a framework combining a neural network and RL to address this issue. Experiments showed that their approach works well in terms of solving classic combinatorial optimization problems such as TSPs and KPs. This provided a way to solve combinatorial optimization problems with DRL. Following this work, many new methods based on the PN architecture have been successively proposed at artificial intelligence summits aiming at TSPs [19], [20], vehicle routing problems (VRPs) [21], [19], [16], [22], [23], KPs [24], the max-cut problem [25] and other combinatorial optimization problems in the past three years and have achieved satisfactory effects. Aside from the PN architecture, graph neural network and attention layer models are also used to solve combinatorial optimization problems [26]. Dai et al. [27] first studied combinatorial optimization problems such as minimum vertex cover (MVC) problems and TSPs by combining graph neural network and DRL methods. The graph neural network was used to estimate the Q value of each optional node, according to which the node inserted next could be determined with a greedy strategy. This tactic was repeated until inserted nodes constituted a complete solution. Wouter Kool et al. [16] proposed a model based on attention layers and trained it by using REINFORCE with baselines to solve common combinatorial optimization problems. The attention mechanism used in their work instead of recurrence (long short-term memory (LSTM)) is more suitable for problems without requirements regarding the order of the input nodes, increasing learning efficiency. The multihead attention mechanism in their work allows nodes to share relevant information over different channels, which is important for choosing nodes. They performed experiments with the same hyperparameters on problems including a TSP, a VRP, an OP and a prize collecting TSP (PCTSP) and obtained high-quality solutions. Based on attention research, Ricardo Gama et al. [15] proposed a modified PN architecture to address the OP with time windows (OPTW). They utilized a recursive attention model that relied on a transformer block with dynamic graph self-attention, and RL was used to train this model. Experimental results showed that their approach generally outperforms the ILS method [2], one of the most commonly used heuristics in OPTW research, and can generate solutions in seconds once trained.

Successful applications of DRL methods to combinatorial optimization problems, especially TSPs, make it feasible to solve OPs by decomposition. According to the idea of the DM mentioned before, once one DRL model (as the TSP solver) is trained, it can immediately generate a solution (node access sequence) based on the nodes selected by the KP solver, as well as the length of the route. The KP solver, which can be one kind of heuristic or learning heuristic, then adjusts the selected nodes according to nodes' values and routes' lengths. Adjusting the solutions iteratively eventually results in a good solution for the given OP. Since the TSP solver can provide solutions immediately, the complexity of the OP can be reduced nearly to that of a KP, which is a landmark finding for large-scale OPs and their variants. Compared with solving an OP directly by DRL, the DM combining a heuristic and DRL uses fewer training resources and has a stronger generalization ability, which means that the DM is more feasible in practical problems, especially with large-scale and dynamic data. While the evaluation time of the DM may reach the minute level, it is much faster than traditional heuristics and still acceptable.

In this paper, we decompose an OP into a KP and a TSP and apply the evolutionary algorithm (EA) as the KP solver and the DRL as the TSP solver. The framework in this paper is thus called EA-DRL. Specifically, we propose a dual-population coevolutionary algorithm (DPCA) for the KP module. Different from general EAs such as the second-generation nondominated sorting genetic algorithm (NSGA-II), this method simultaneously maintains one feasible population and one infeasible population while evolving, where the goal is maintain population diversity and prevent the algorithm from falling into a local optimum while dealing with constraints. A greedy strategy (GS) is used for population initialization to accelerate the evolution of the population. To effectively solve the TSP module, we improve the PN with an attention mechanism and dynamic information (named the dynamic pointer network (DYPN)) and train it via the REINFORCE method. For specific cases, the pretrained model can be retrained on small samples to further improve its performance. The experimental results prove the effectiveness and strong generalization ability of our proposed framework.

In conclusion, the contributions of this work can be concluded as follows.

- A decomposition framework called EA-DRL based on the EA and DRL is proposed for solving OPs. Compared with existing algorithms, EA-DRL performs better on large-scale instances, with high generalization ability and lower training costs.
- An improved evolutionary algorithm (DPCA) is introduced; it can deal with strong constraints and greatly improves population diversity during the process of evolution. Feasible and infeasible populations are maintained together. While the feasible solutions evolve towards better objective function values, the infeasible solutions evolve towards reducing constraint violations. This strategy effectively prevents the solutions from falling into local optimum.
- The conventional PN is improved. In detail, beyond incorporating an attention mechanism into the decoder, node distance information is also dynamically integrated into the attention layer, helping with the calculation of the attention vector.
- Extensive experiments are conducted to validate the learning ability, evaluation performance and generalizability of the proposed approach. The performance of the transfer learning method on pretrained models is also discussed. The experimental results demonstrate the great optimization ability and generalization ability of our framework.

The rest of this paper is structured as follows. Section II describes our proposed EA-DRL framework, which includes the DPCA module and the DYPN module, in detail. Then, Section III introduces the REINFORCE training method. The experimental setup is specified in Section IV, and the experimental results are analyzed in Section V. The last section gives the conclusion as well as future directions.

II. Proposed Model

A. General Framework

In this section, we propose to solve the OP by decomposing it into a KP and a TSP and innovatively solve it with an effective framework combining an EA and a DRL method: EA-DRL. The general framework of EA-DRL is presented in Algorithm 1. While the EA works as the KP solver for selecting nodes of interest, the DRL model is in charge of solving the TSP to obtain a Hamiltonian path based on the previously selected nodes. Afterwards, this route length is fed back to the KP solver, and the populations then evolve according to their fitness. The last Hamiltonian path is exactly the solution of the OP.

One obvious advantage of EA-DRL is its modularity and simplicity for users. Any heuristic can be deployed as the KP solver (such as the EA here), and other novel DRL-based TSP solvers [16], [15] can also be integrated into this framework. In addition, the framework is also suitable for all kinds of variants of the OP simply by adding appropriate constraints to the KP solver or the TSP solver.

In this paper, we propose the DPCA as the KP solver and the DYPN as the TSP solver; they are described in detail later.

Algorithm 1 General Framework of EA-DRL

Input: instance set $\mathcal{M}$, maximum number of generations $MaxGen$, population size N

Initialize $gen \leftarrow 1$
Train the DRL model for the TSP: $DRLModel \leftarrow REINFORCE(\mathcal{M})$
$Pop \leftarrow Initialization(N)$
while $gen \leq MaxGen$ **do**
  $Route, Length \leftarrow DRLModel(Pop)$
  $Pop \leftarrow EA(Pop, Route, Length, N)$
  $gen \leftarrow gen + 1$
end while
$Route, Length \leftarrow DRLModel(Pop)$
$Arc \leftarrow UpdateArc(Pop, Route, Length)$

B. DPCA

As one of the most classic combinatorial optimization problems, the KP [28] has been researched for decades. Various mature algorithms, including exact algorithms [29], [30], [31] and heuristic evolutionary algorithms [32], [33], [34], [35], are already available for solving it. While the exact algorithms can obtain more accurate solutions, the heuristics work better and faster on large-scale problems. However, for heuristics, the greatest challenge when solving a KP is the processing of constraints. Several general constraint handling techniques are available: the principle of penalty functions [36], [37], [38], [39], infeasible solution repair method [34], [35], the stochastic ranking method [40], the ϵ-constrained method [41] and the tournament selection method based on feasibility [42]. While these approaches may be effective in specific situations, they also possess some shortcomings that make them unsuitable for our problem. The principle of penalty functions, the stochastic ranking method and the ϵ-constrained method have high parameter setting requirements, and the repair operators cost much time, especially in large-scale instances. Although the tournament selection method requires no hyperparameters and works fast, it evolves in the direction of feasible solutions, which results in a massive population diversity loss.

In this study, we propose a DPCA for solving the KP module; this algorithm can perfectly handle the problems mentioned above. Its main idea is to divide the population into one feasible population and one infeasible population while maintaining them simultaneously. In each generation, we keep their population size as consistent as possible. While the feasible population is in charge of searching for the optimal solution, the infeasible population aims to provide diverse genes to prevent the feasible population from falling into local optimum. The framework of the DPCA is illustrated in Algorithm 2, which is similar to the general framework of NSGA-II [43], including the following parts: population initialization, mate selection, offspring generation and environmental selection. Similar to other heuristics, a binary coding mode is used here. Among the employed operators, the stochastic universal sampling method is used as the $MateSelection$ operator, which randomly samples one individual from the current population Pop N times. For offspring generation,

we choose the two-point crossover method (Xovdp) as the $Crossover$ operator with a crossover probability of P_c and the binary chromosomes mutation method (Mutbin) as the $Mutation$ operator with a mutation probability of P_m. For the two-parent matched individuals, Xovdp randomly sets two intersections and exchanges the gene segments according to the crossover probability P_c. Mutbin changes every gene in the chromosomes according to the mutation probability P_m. The population initialization method, as well as the dual-population selection operator, are stated in detail below. Afterwards, the $UpdateArc$ operator selects the optimal feasible individual Arc from the population.

Algorithm 2 General Framework of the DPCA

Input: Maximum number of generations $MaxGen$, population size N

```
Initialize gen ← 1
Pop ← Initialization(N)
while gen ≤ MaxGen do
    MatingPool ← MateSelection(Pop)
    Off ← Crossover(MatingPool)
    Off ← Mutation(Off)
    Pop ← DualPopSelection(Pop, Off, N)
    gen ← gen + 1
end while
Arc ← UpdateArc(Pop)
```

1) Population Initialization: The quality of the initial population can largely influence the evolution speed. In this paper, we propose a greedy strategy for population initialization. For each individual, this method selects nodes in steps. At each step, one node is sampled according to one probability vector until no nodes can be added while still satisfying the constraint. To calculate the probability vector, we first define a value density vector $I^i = \{I^i_j, j = 1, \ldots, N\}$ for each node i based on the Euclidean distance matrix $T = \{t_{ij}, i, j = 1 \ldots, N\}$ and the value vector $S = \{s_j, j = 1 \ldots, N\}$. The formulation of the value density I^i_j is shown in (1).

$$I^i_j = s_j / t_{ij}; \quad \forall i = 1, \ldots, N; \forall j \in U \tag{1}$$

This indicates how worthy node j is of being selected next when the last node selected is i. The higher the score of I^i_j for node j is, the more likely j is to be selected in that step. Notably, considering that nodes cannot be visited repeatedly, visited nodes must be excluded. The set of unreached nodes is presented as U. The normalization of this indicator produces a probability vector, as formulated in (2). The next node is then sampled according to this probability vector.

$$P^i = \mathrm{softmax}(I^i); \quad \forall i = 1, \ldots, N \tag{2}$$

2) Dual-Population Selection: For the environmental selection component, we propose a method called dual-population selection. By calculating each individual's route length through the DYPN, the whole population including the offspring and parents can be first divided into feasible and infeasible populations. In each evolution generation, the next-generation population is selected from these two populations. Ideally, $50\%N$ of the feasible individuals and $50\%N$ of the infeasible individuals form the new population; however, as the variance of the population size during evolution is uncontrollable, this requirement can only be satisfied as well as possible. Each individual is selected via the use of the tournament selection method with an elitism strategy [43] according to the individual fitness levels. The fitness $\boldsymbol{F}$ is defined as follows.

$$\boldsymbol{F} = a * \boldsymbol{Obj} + b * \boldsymbol{Cv} + c \tag{3}$$

$$\boldsymbol{Cv} = \begin{cases} T_{real} - T_{max} & T_{max} < T_{real} \\ 0 & T_{max} \geq T_{real} \end{cases} \tag{4}$$

where $\boldsymbol{Obj}$ is the objective function value and $\boldsymbol{Cv}$ (≥ 0) is the violation of the constraint. a, b and c are hyperparameters. T_{real} represents the total length of the tour. Since feasible solutions do not violate constraints, $\boldsymbol{Cv} = 0$ for feasible solutions. Note that since $a > 0$ and $b < 0$, the larger $\boldsymbol{Obj}$ is or the smaller $\boldsymbol{Cv}$ is, the larger the fitness $\boldsymbol{F}$.

While individuals in the infeasible population cannot be selected as the final solution, they continuously provide the feasible population with diverse genes that may be effective. This helps prevent solutions from falling into local optimum. Such a constraint handling method is general and easy to use and works quickly and effectively.

C. DYPN

After the nodes are selected, a Hamiltonian path is immediately needed. To solve this problem (the TSP) effectively, we propose a deep learning technique with dynamic embeddings, similar to the improved PN proposed by Nazari [19]. The model is formally described as follows. Taking a TSP instance k with N cities as an example, feature $\mathbf{x}_i$ of city i is defined by its location, i.e., its x-coordinate and y-coordinate. A solution $\boldsymbol{\pi} = (\pi_1, \ldots, \pi_N)$ is a permutation of all the cities. It is worth mentioning that the position of the depot in the permutation is unimportant, as the path can always be a loop. The DYPN takes city locations $\{\mathbf{x}_i\}$ as inputs and outputs the city visitation sequence $\boldsymbol{\pi}$. With the utilization of the probability chain rule, a policy $p(\boldsymbol{\pi}|k)$ for selecting $\boldsymbol{\pi}$ given instance k can be described as follows:

$$p_\theta(\boldsymbol{\pi} \mid k) = \prod_{t=1}^{N} p_\theta\left(\pi_t \mid k, \boldsymbol{\pi}_{0 \sim t-1}\right) \tag{5}$$

where $\boldsymbol{\theta}$ represents the model parameters. It is certain that when the parameter set $\boldsymbol{\theta}^*$ is optimal, the model can generate the optimal tour $\boldsymbol{\pi}^*$ for the given instance.

We still follow the encoder-decoder architecture for modeling purposes. The encoder is used to produce the embeddings of all nodes, including static embeddings and dynamic embeddings. While the static embeddings contain the structural patterns of the problem, the dynamic embeddings describe the dynamic patterns. The decoder produces the node access sequence $\boldsymbol{\pi}$ by selecting nodes individually with the node embeddings as inputs. In this work, the encoder is a set of embeddings, and the decoder consists of a recurrent neural network (RNN) and a context-based attention mechanism.

1) Encoder: The encoder is structured to present each city (mainly its geographic location information) in this work. While RNNs [18] and multihead attention (MHA) [16], [15], [44] mechanisms are commonly used as encoders in deep learning techniques, their complexity is still unsatisfactory. In fact, the use of an RNN in the encoder is actually unnecessary, as we do not need to pay attention to the sequential TSP input information here. To simplify the complexity of our model, 1-dimensional convolution layers are used to map the inputs to a D-dimensional vector space. In each 1D convolution layer, the number of in-channels is the input length, the number of filters is set as D, which is also the number of out-channels, and the kernel size is 1 for each filter. The schematic diagram is shown in Fig. 1. Notably, multiple embeddings are utilized for different input elements, but they are shared among these inputs. Different from the pure node embedding encoder [19], we embed not only the static features of inputs such as their location information but also their dynamic situations, which are described as dynamic distances. Let us define the input set as $X = \{x^i, i = 1, \ldots, N\}$, in which each input x^i is a sequence of tuples $\{x_t^i = \left(s^i, d_t^i\right), t = 0, \ldots, T\}$, where s^i and d_t^i are the static and dynamic elements, respectively. The static embeddings and dynamic embeddings are stated in detail as follows.

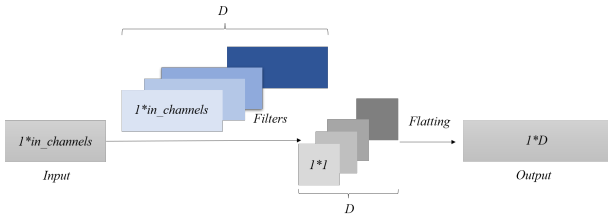

Fig. 1. The structure of a 1D convolution layer. D filters with sizes of $kernel\_size * in\_channels$ are used to deal with the input features (with sizes of $1 * in\_channels$). The D filters generate D feature maps with sizes of $1 * 1$. A flattening layer is used here to flatten these D feature maps to a D-dimensional vector, which is used as the output.

Static embeddings. A static embedding represents the static feature s^i of a city i, which is defined as its location in this work. Considering that the location of each city is a 2-dimensional vector, the input length of each static embedding is 2. Therefore, the static embedding is modeled as the 1D convolution layer described before, and the 2-dimensional location input s^i is mapped to a D-dimensional vector $\bar{s}^i$ ($D = 128$ in this work), as shown in Fig. 2 (a). For all N nodes, the static embeddings are set as $\bar{s} = \{\bar{s}^i, i = 1, \ldots, N\}$.

Dynamic embeddings. In fact, the static embeddings $\{\bar{s}^i, i = 1, \ldots, N\}$ contain the full details of the TSP, and they are sufficient for the neural network to learn a policy $\boldsymbol{\pi}$. However, aimless parameter learning in large-scale problems is difficult. Considering that the distance information between nodes plays an important role in planning paths via steps, we introduce the Euclidean distances $\{E_t^i, i = 1, \ldots, N\}$ between the node decoded in decoding step t and the other nodes $\{i = 1, \ldots, N\}$ as the dynamic embeddings. We also apply data normalization to make the learning process more effective. In this work, we address each Euclidean distance vector $\{E_t^i, i = 1, \ldots, N\}$ by using a normalization method called *negative maximum-minimum normalization*. Supposing that its maximum and minimum values are E_t^{max} and E_t^{min}, respectively, the dynamic feature d_t at timestep t can be formulated as (6). Note that unlike in the general *maximum-minimum normalization* method, we use $E_t^{max} - E_t^i$ instead of $E_t^i - E_t^{min}$ as the molecule to pay more attention to the nodes that are closer to the current node.

$$d_t = \left\{ \frac{E_t^{max} - E_t^i}{E_t^{max} - E_t^{min}}, i = 1, \ldots, N \right\} \tag{6}$$

As in the embedding process of static embeddings, a 1D convolution layer is used to map a dynamic feature d_t into a dynamic embedding $\bar{d}_t$, as shown in Fig. 2 (b). Since d_t^i is a value, the numbers of in-channels in these dynamic embeddings are 1. Unlike the application situation of the static embeddings, the dynamic embeddings are used only in the attention layer and not in the RNN to simplify the calculations.

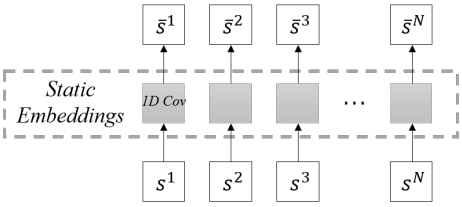

(a) The process of static embedding.

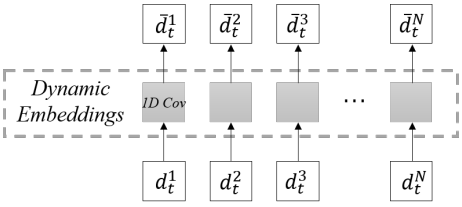

(b) The process of dynamic embedding at timestep t.

Fig. 2. The processes of embedding.

2) Decoder: The decoder is composed of two parts: an RNN and a context-based attention module (including an attention layer, a context embedding layer, a log-probability layer and an inference layer). While the RNN is in charge of remembering each output of decoding, the attention module is used to calculate the probability of node selection. In detail, Fig. 3 illustrates the decoder structure as well as the decoding process.

The decoder generates outputs in steps. For timestep $t \in (1, \ldots, N)$, the RNN takes the static embedding $\bar{s}^{\pi_{t-1}}$ of the last decoded node π_{t-1} ($\bar{s}^{\pi_0}$ is set as the static embedding of a 2-dimensional zero vector) and its last output h_{t-1} (if $t > 1$) as inputs and eventually outputs h_t. After that, the attention layer is used to measure how relevant every input node might be in this decoding step. While the inputs include the memory state h_t of the RNN, all static embeddings $\bar{s}$ and the dynamic embeddings $\bar{d}_t$ at timestep t ($\bar{d}_1$ is set as the dynamic embedding of a 1-dimensional zero vector), the output is a variable-length alignment vector a_t. The context embedding layer is then used to produce a context vector c_t, based on a_t and $\bar{s}$. Afterwards, the log-probability layer

and the inference layer are employed to compute the output probabilities $p_\theta\left(\pi_t \mid k, \pi_{0\sim t-1}\right)$ in (5) and choose the node to be visited in this step, respectively. These patterns are described in detail as follows.

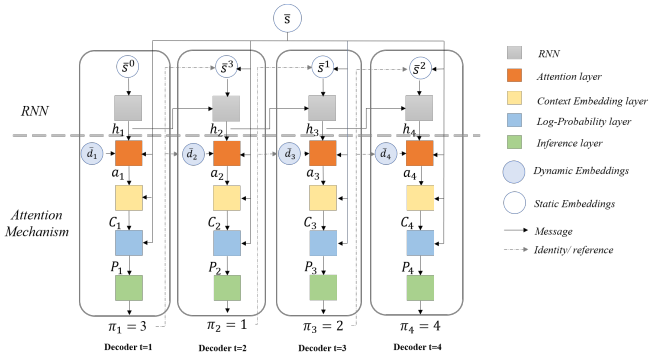

Fig. 3. The process of decoding. The decoder takes both the static and dynamic embeddings as inputs, while the dynamic embeddings are only used in the attention layer. The example shows how a tour $\boldsymbol{\pi} = (3, 1, 2, 4)$ is constructed.

RNN. As RNNs are effective for processing sequential data, we use a gated recurrent unit (GRU) [45], a classic variant of RNNs, to save the information of the visited nodes in this work. The GRU takes the static embedding of the previous node $\bar{s}^{\pi_{t-1}}$ and its last memory state h_{t-1} (if $t > 1$) as inputs and outputs a new memory state h_t. This can be formulated as (7).

$$h_t = f_{GRU}\left(\bar{s}^{\pi_{t-1}}, h_{t-1}\right) \tag{7}$$

Since no node is selected in step $t = 1$, $\bar{s}^{\pi_0}$ is initialized by the embedding of a 2-dimensional zero vector.

Attention layer. The attention layer is proposed to generate an alignment vector a_t at each timestep t, specifying the importance of each node in the current decoding step. a_t can be computed as in (8).

$$a_t = \operatorname{softmax}\left(u_t\right) \tag{8}$$

where

$$u_t = v_a^T \tanh\left(W_a\left[\bar{s}; \bar{d}_t; h_t\right]\right) \tag{9}$$

Here, ";" represents the concatenation of two vectors, and v_a and W_a are learnable parameters.

Context embedding layer. This layer is used to compute a vector called the context, which represents the weighted static embeddings with a_t as their weights. Context is defined as follows:

$$c_t = a_t \bar{s} \tag{10}$$

Log-probability layer. With the combination of the static embeddings $\bar{s}$ and the context c_t as inputs, the log probability mentioned in (5) for each node can be calculated as in (11).

$$p_\theta\left(\pi_t \mid s, \boldsymbol{\pi}_{0\sim t-1}\right) = \operatorname{softmax}\left(\tilde{u}_t\right) \tag{11}$$

where

$$\tilde{u}_t = v_c^T \tanh\left(W_c\left[\bar{s}; c_t\right]\right) \tag{12}$$

Here, v_c and W_c are learnable parameters.

Inference layer. The inference layer is used to choose the node to be decoded based on the log probabilities $p_\theta\left(\pi_t \mid s, \boldsymbol{\pi}_{0\sim t-1}\right)$. While four general inference methods are available, including *sampling search*, *greedy search*, *beam search* and *active search* approaches, as illustrated by Gama [15], we choose two of them in our inference layer. Specifically, we use a *sampling search* during the model training stage to increase the exploration ability of the model and a *greedy search* during validation to obtain the solution in a short period of time. The sampling search process samples one node according to the probability vector $p_\theta\left(\pi_t\right)$ at step t and eventually constructs one solution of the TSP. In contrast, the greedy search directly selects the node with the highest probability for each step.

In conclusion, the model is therefore composed of the above encoder and decoder. The 1D convolution layers are used as the embeddings in the encoder to map the node inputs to high-dimensional vectors. In particular, dynamic embeddings are introduced based on the distances between nodes. The decoder is designed with an RNN and a context-based attention mechanism to make decisions sequentially until all the cities are visited. The order of the selected cities determines the final solution $(\pi_1, \pi_2, \ldots, \pi_N)$.

III. Training with the REINFORCE Algorithm

The REINFORCE algorithm [46], a well-known policy gradient approach, is used here to train the DYPN. For a stochastic policy $\boldsymbol{\pi}$ parameterized by θ and ϕ, REINFORCE uses estimates of rewards and learns to improve itself by a *state-action-reward* tuple. Two networks are contained in the REINFORCE algorithm: an actor network and a critic network. For any problem instance k, while the actor provides a node access sequence (solution) as well as the solution reward $L(\boldsymbol{\pi})$ based on the given policy $\boldsymbol{\pi}$, the critic is in charge of giving an estimated reward $V(k; \phi)$, where ϕ is the parameter set of the critic. In this paper, the actor network is exactly the stated DYPN model, and the critic is formed by two dense layers with rectified linear unit (ReLU) activation and one linear layer with a single output; the inputs are static and dynamic embeddings. The training loss is defined as (13), and its gradient is formed as (14):

$$\mathcal{L}(\boldsymbol{\theta} \mid k) = E_{p_{\boldsymbol{\theta}}(\boldsymbol{\pi}|k)}[L(\boldsymbol{\pi}) - V(k; \phi)] \tag{13}$$

$$\nabla\mathcal{L}(\boldsymbol{\theta} \mid k) = E_{p_{\boldsymbol{\theta}}(\boldsymbol{\pi}|k)}\left[(L(\boldsymbol{\pi}) - V(k; \phi))\nabla \log p_{\boldsymbol{\theta}}(\boldsymbol{\pi} \mid k)\right] \tag{14}$$

From the problem set $\mathcal{M}$ with a probability distribution $\Phi_{\mathcal{M}}$, we can sample M instances as the training instances during each training epoch. Algorithm 3 summarizes the training process. We first initialize the actor and critic networks with random parameters θ and ϕ, respectively. In each training epoch, we draw M instances according to the given distribution $\Phi_{\mathcal{M}}$. For each instance k_m, a solution $\boldsymbol{\pi}$ is generated sequentially by the actor, and its reward $L^m(\boldsymbol{\pi})$ can be calculated as well. At the same time, we adopt the critic to calculate the corresponding approximation reward $V(k_m; \phi)$ for instance k_m. After the rewards and approximated rewards are counted for all M instances, we can update the parameters of both the actor and the critic, as shown in steps $12 - 14$. Such parameter updates last for N_{epoch} epochs.

Algorithm 3 Training the Algorithm by using REINFORCE

Input: number of problem instances $\mathcal{M}$, number of training epochs N_{epoch}

Initialize the actor network with random weights θ and the critic network with random weights ϕ
for $epoch = 1 : N_{epoch}$ **do**
  reset gradients: $d\theta \leftarrow 0, d\phi \leftarrow 0$
  sample M instances according to $\Phi_{\mathcal{M}}$
  for instance $k_m = k_1, \ldots, k_M$ **do**
    for step $t = 1 : N_{step}$ **do**
      $\boldsymbol{\pi}_t \leftarrow p_{\boldsymbol{\theta}}(k_m, \boldsymbol{\pi}_{0 \sim t-1})$.
    end for
    compute reward $L^m(\boldsymbol{\pi})$
    compute estimated reward $V(k_m; \phi)$
  end for
  $d\theta \leftarrow \frac{1}{M} \sum_{m=1}^{M} \left(L^m(\boldsymbol{\pi}) - V(k_m; \phi)\right) \nabla_{\boldsymbol{\theta}} \log p_{\boldsymbol{\theta}}(\boldsymbol{\pi} \mid k_m)$
  $d\phi \leftarrow \frac{1}{M} \sum_{m=1}^{M} \nabla_{\boldsymbol{\phi}} \left(L^m(\boldsymbol{\pi}) - V(k_m; \phi)\right)^2$
  Update $\boldsymbol{\theta}$ using $d\theta$ and $\boldsymbol{\phi}$ using $d\phi$
end for

IV. Experimental Setup

All experiments are conducted on a PC with an AMD 8-Core R7-5800H CPU @3.2 GHz, 16 GB of RAM and a single RTX 3060 GPU. The code is written in Python 3.8 and will be made open access later for the convenience of experimental reproduction and further research. Additionally, the comparison algorithms are also written and run in the same environment. This section illustrates the experimental setup, including the instance setups, model hyperparameters and evaluation procedure.

A. Test Instances

In the training phases of the DRL models, we randomly generate 1280000 TSP instances with 20, 50 and 100 nodes, and the location of each node is chosen uniformly from a unit square $[0, 1] * [0, 1]$ with a random seed of 1234. It is worth noting that the capacity and node score parameters are not required in the training stage of our DYPN, since it only pays attention to the TSP. However, the training processes of the models in [16] and [15] requires capacity parameters as well as the node score distribution, which greatly limits the generalization abilities of these models. During the testing phase, OP instances with different scales and capacity constraints are generated, as shown in TABLE I, to test the algorithmic performance under different problem sizes. While the data distribution is the same in both the training and testing phases, the random seed in the test instances is set as 12345. The node scores obey a uniform distribution in the range (0,1).

B. Hyperparameters

The hyperparameters of the models in this paper for both training and evaluation are listed in TABLE II. In the training phase of the DRL model, we set 10 as the number of epochs and train for 1280000 instances in each epoch. Notably, the number of epochs here is rather small compared with that utilized by Kool's model [16], whose effective parameter is 100. Since the complexity of the TSP model is much smaller than that of the OP model, through the decomposition-based method developed in this paper, we can much more easily train an effective DRL model in less time. The batch size during training is dynamically set from 32 to 1024 because of the limited memory of the PC. Regarding the other hyperparameters, we use 128-dimensional node embeddings and an encoder-decoder with 128 hidden units. The models are trained via the Adam optimizer [47] with a learning rate of 0.0001 and dropout rate of 0.1. In the DPCA module, the population size is set to 100, and the maximum number of generations is 60. In addition, the probabilities of crossover and mutation are set to 0.9 and 0.01, respectively.

TABLE I
Test instances

Problem Name	Nodes	Capacity
OP20	20	2,3,4
OP30	30	2,3,4
OP50	50	3,4,5
OP80	80	4,5,6
OP100	100	5,6,7
OP150	150	8,9,10
OP200	200	9,10,11

TABLE II
Hyperparameter configurations

DRL		EA	
Hyperparameters	**Value**	**Hyperparameters**	**Value**
No. of epochs	10	Population size	100
No. of instances	1280000	Max No. of generations	60
Hidden dimensions	128	Probability of crossover	0.9
Optimizer	Adam	Probability of mutation	0.01
Learning rate	1e-4		
Dropout rate	0.1		

C. Evaluation Procedure

We first analyze the learning ability of our DRL model during training in comparison with other recent state-of-the-art deep learning baselines: the PN[1] [19] and the attention model (AM)[2] [16]. After that, we randomly generalize 21 OP instances with different scales and capacities, as listed in TABLE I. We compare our EA-DRL model with the AM, one classic evolutionary algorithm (the GA), and one heuristic method (the GS) in terms of their OP solving abilities. The GA and the GS[3] have also been used as comparison algorithms in past works [16].

For each problem, we also report the 'best possible solution' via Gurobi [48], a commercial optimization solver. To facilitate the comparison, the hyperparameters used in these algorithms are as consistent with those of our framework as possible; this is illustrated in detail later. In addition, we introduce the fine-tuned DRL model (FT-DRL) for each test instance based on the previously trained global DRL model and evaluate its

[1]https://github.com/mveres01/pytorch-drl4vrp
[2]https://github.com/wouterkool/attention-learn-to-route
[3]https://github.com/mc-ride/orienteering

performance on the same instance. Fine-tuning occurs for 5% of the regular training instances (i.e., 64000 instances). While the DRL models are trained on 20, 50 and 100 nodes, the EA-DRL framework is tested on 20, 30, 50, 80, 100, 150 and 200 nodes; the generalization abilities of the models are discussed as well.

V. Experimental Results and Discussion

In this section, the learning ability, evaluation performance and generalization of our framework are demonstrated in comparison with those of other models.

A. Learning Abilities of DRL Models

While deep learning methods are convenient and efficient for use, the model training process is always time-consuming. In this part, we first evaluate the learning ability our DRL model, the DYPN, during training in comparison with two other famous models: the PN and AM. Based on the same training parameters, we train these models. Taking the instance with 20 nodes as an example, we set the instance size as 1280000, the batch size as 1024 and the number of training epochs as 49. Notably, since the DYPN and PN are for designed solving the TSP but AM is meant for the OP, the cost for evaluating the AM is different from those of the DYPN and PN. While the average predicted tour length is used as the cost for evaluating the DYPN and PN, the negative average predicted tour score is employed for the AM. We compare the training costs of the DYPN with PN to demonstrate how the difficulty of model training is reduced and the effect is improved by the introduction of dynamic information, and we also compare the DYPN with the AM to show the advantage of our model with respect to convergence.

Fig. 4 shows the performance of the DYPN and PN when training for 12500 batches (10 epochs). To show the gap between these models more clearly, we separate the curves for the initial 2000 batches and the last 500 batches, as shown on the right. Notably, our model outperforms the PN in terms of both the convergence speed and the final cost, which shows the effectiveness of the dynamic information in the PN model. This is understandable since the dynamic information dynamically provides extra features to the DRL agent, and the agent can make decisions with heuristic guidance.

Fig. 5 shows the performance of the DYPN and AM in the training stage with more training batches (i.e., 61250 batches or 49 epochs). While we cannot directly compare the final costs of the trained models, the training performance in terms of convergence is apparent. Affected by the varied node scores, the AM designed for the OP is difficult to train to achieve convergence. The OP solutions of different instances may be greatly different. In comparison, the training process of the DYPN for the TSP does not need to consider the node score data, enabling it to converge quickly. While the AM must be trained for 100 epochs [16], it is sufficient to train the DYPN for only 10 epochs.

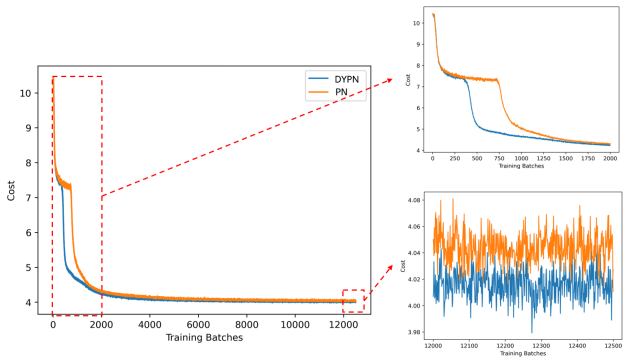

Fig. 4. Cost changes along with the number of batches in the training stage for the DYPN and PN.

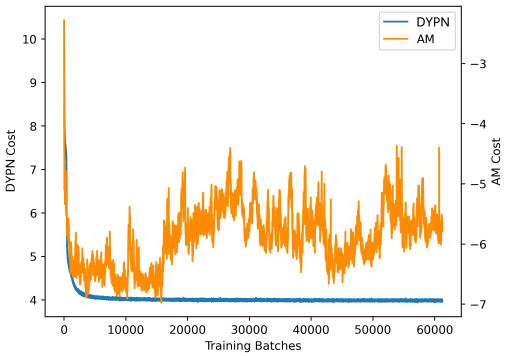

Fig. 5. Cost changes along with the number of batches in the training stage for the DYPN and AM.

B. Model Performance on Test Set

To evaluate the model performance, we set several OP instances with different scales and capacities, as listed in TABLE I. Limited models trained on small-scale instances (Node20, Node50, and Node100) are used to evaluate the performance of the DYPN and AM. Following the settings in [16], we train the AM for 100 epochs containing instances with 20 nodes at capacity 2, 50 nodes at capacity 3 and 100 nodes at capacity 4 (called AM20, AM50, and AM100, respectively). The DYPN models are trained for 10 epochs with instances containing 20 nodes, 50 nodes and 100 nodes (called DYPN20, DYPN50, and DYPN100, respectively). Fig. 6 shows the validation of DYPN20, DYPN50 and DYPN100 based on the corresponding datasets randomly generated on seed 1234. The average tour lengths of the validation results are 3.95, 6.08 and 8.51, respectively.

Empirically, since a large gap between the instance sizes of training and testing may result in great performance degradation for all deep learning methods, we dynamically choose models trained on different instances for different test instances. For the AM models, it is intuitive that we should match each test instance with the AM model whose training instance has the closest size. What is different about the DYPN models is that since the test instances are designed for the OP, gaps may be present between the test instance sizes and the

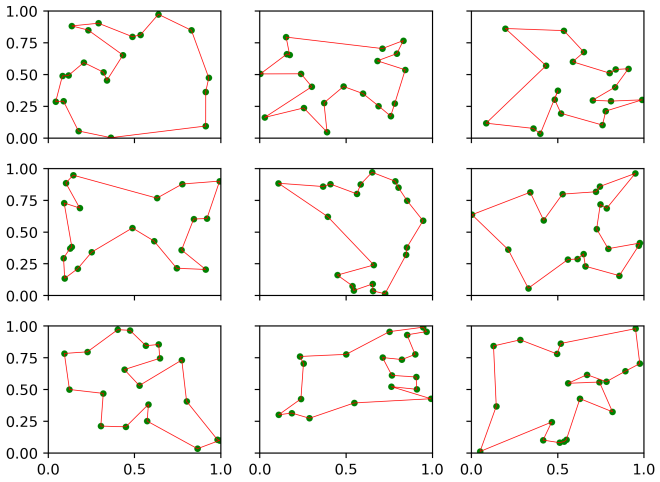

(a) Validation of DYPN20 (3.95)

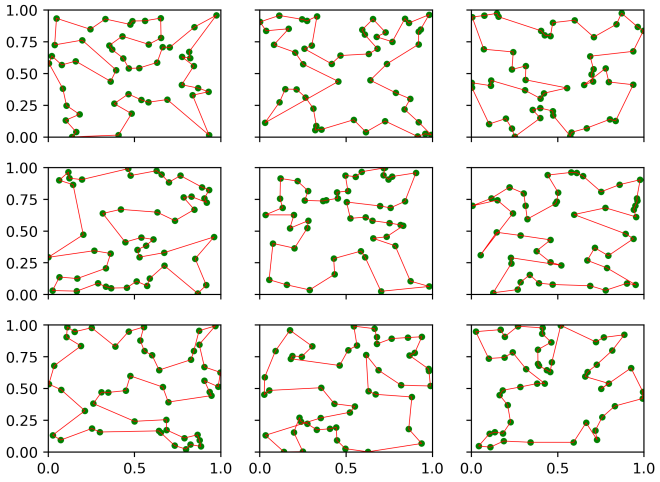

(b) Validation of DYPN50 (6.08)

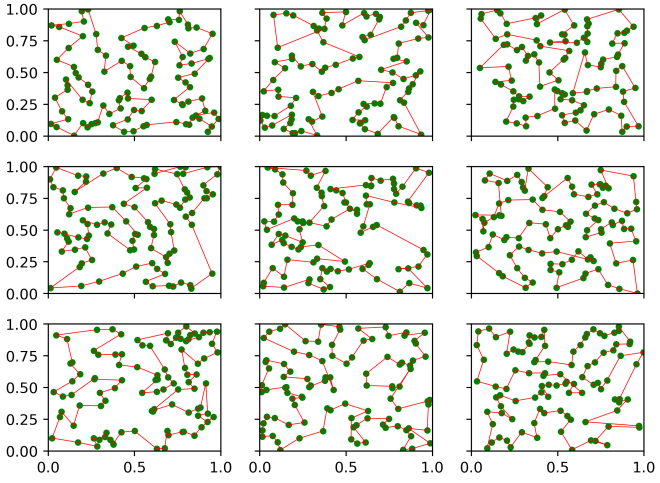

(c) Validation of DYPN100 (8.51)

Fig. 6. Validation results of the trained DYPN models on TSP instances.

TABLE III
SELECTED DRL MODELS FOR THE TEST INSTANCES

Test Size	Capacity	1.3*G	DYPN	AM
OP20	**2** **3** **4**	<20	DYPN20	AM20
OP30	**2** **3** **4**	<30	DYPN20	AM20
OP50	**3** **4** **5**	23 24 30	DYPN20	AM50
OP80	**4** **5** **6**	24 34 42	DYPN20 DYPN50	AM100
OP100	**5** **6** **7**	47 52 64	DYPN50	AM100
OP150	**8** **9** **10**	83 97 111	DYPN100	AM100
OP200	**9** **10** **11**	99 120 128	DYPN100	AM100

training instance sizes of the DYPN models. We propose a method to adaptively select the DYPN models according to the solutions calculated by the greedy algorithm; this is done for the population initialization illustrated before. Considering room for optimization, supposing that the number of nodes selected in the greedy solution is G, we set the baseline size as $\lfloor 1.3 * G \rfloor$, and we can choose the DYPN model whose training instance size is closest to this value. The models selected for all test instances are listed in TABLE III. We use the total scores of the generated tours to evaluate the models. Apart from that, the running time, as well as the gaps between these models and the possible best solver (Gurobi), are also shown. The gaps are defined as in(15).

$$Gap = \frac{S_g - S_m}{S_g} * 100\% \tag{15}$$

where S_g is the score of the solution calculated by Gurobi in 300 seconds and S_m is the score of the solution calculated by some other model.

TABLE IV shows the performance of the compared approaches on the test instances. Notably, in consideration of the randomness in evolutionary algorithms, we run the GA, EA-DRL and the fine-tuned EA-DRL (EA-DRL-FT) 10 times on each test instance and take the average score for comparison.

For the heuristics used in this work, it is obvious that the traditional EAs such as the GA work poorly on the OP, and their time consumptions increase sharply as the problem scale increases. Notably, the design of evolution strategies are vital. One greedy strategy designed for the OP is compared here. While very large gaps are present relative to the performance of Gurobi, the proposed approach outperforms the GA in terms of both accuracy and speed.

As the results show, deep learning methods perform better overall. In detail, we compare our framework (EA-DRL) with one recent advanced DRL model (the AM). It can be seen that the AM has a great advantage in computing speed and can generate solutions in seconds once the model is trained. Due

TABLE IV
EVALUATION RESULTS OF THE COMPARED MODELS

Node	Capacity	Gurobi (300 s)		GA			Greedy			DRL			EA-DRL			EA-DRL-FT		
		score	time(s)	score	gap	time(s)	score	gap	time(s)	score	gap	time(s)	score	gap	time(s)	score	gap	time(s)
	2	5.6	1	5.60	0.00%	10	4.61	17.68%	0	5.38	3.93%	3	5.60	**0.00%**	105	5.60	**0.00%**	248
20	**3**	7.56	0	7.16	5.34%	16	7.20	4.76%	0	6.72	11.11%	2	7.56	**0.00%**	123	7.56	**0.00%**	313
	4	7.91	0	7.63	3.50%	21	7.91	0.00%	0	7.55	4.55%	5	7.91	**0.00%**	134	7.91	**0.00%**	357
	2	9.48	218	9.38	1.05%	23	8.31	12.34%	0	8.90	6.12%	2	9.18	**3.16%**	121	9.11	3.92%	304
30	**3**	13.04	175	11.50	11.84%	37	12.03	7.75%	0	12.56	**3.68%**	2	12.10	7.21%	158	13.00	**0.31%**	404
	4	14.4	300	12.52	13.03%	49	14.11	**2.01%**	0	13.36	7.22%	3	14.01	2.71%	175	14.36	**0.29%**	470
	3	17.84	300	13.57	23.95%	83	15.05	15.64%	0	17.27	**3.20%**	2	16.74	6.18%	180	17.05	4.41%	671
50	**4**	20.95	301	14.56	30.52%	111	19.88	5.11%	0	20.53	**2.00%**	2	20.47	2.29%	213	21.20	**-1.21%**	707
	5	24.31	301	15.90	34.58%	142	23.00	5.39%	0	22.86	5.96%	2	23.86	**1.86%**	256	24.32	**-0.06%**	878
	4	24.03	300	15.71	34.62%	223	20.51	14.65%	1	24.34	**-1.29%**	2	23.21	3.43%	231	25.12	**-4.54%**	728
80	**5**	30.77	300	17.68	42.54%	287	26.05	15.34%	1	30.19	**1.88%**	3	29.90	2.82%	295	31.46	**-2.25%**	988
	6	36.79	300	18.78	48.95%	354	30.78	16.34%	1	33.41	9.19%	3	35.39	**3.82%**	353	35.94	**2.30%**	1214
	5	37.14	300	19.52	47.44%	410	30.38	18.20%	2	34.77	6.38%	3	36.74	**1.07%**	337	37.26	**-0.32%**	1313
100	**6**	42.31	300	20.66	51.16%	512	34.85	17.63%	2	38.37	9.31%	3	42.50	**-0.44%**	396	42.55	**-0.58%**	1433
	7	33.53	300	22.20	33.80%	599	41.81	-24.69%	2	42.34	-26.27%	3	46.32	**-38.13%**	445	47.13	**-40.55%**	1742
	8	67.16	301	25.46	62.09%	1268	59.49	11.42%	7	59.94	10.75%	3	65.78	**2.06%**	622	66.85	**0.46%**	2497
150	**9**	73.88	301	26.88	63.62%	1490	65.59	11.22%	8	67.64	8.45%	4	70.27	**4.88%**	681	71.14	**3.71%**	3909
	10	76.22	301	29.19	61.70%	1705	72.04	5.48%	9	69.72	8.53%	3	71.87	**5.70%**	701	72.09	**5.42%**	4382
	9	83.8	302	28.71	65.74%	2246	72.27	13.76%	16	76.13	9.15%	3	79.43	**5.22%**	782	79.99	**4.55%**	3989
200	**10**	87.66	301	31.47	64.10%	2482	76.25	13.02%	18	80.39	8.29%	3	85.73	**2.20%**	856	85.87	**2.04%**	4790
	11	94.56	301	31.69	66.49%	2798	86.26	8.78%	19	82.81	12.43%	3	87.19	**7.79%**	899	87.23	**7.75%**	5029
AVG GAP		**0.00%**		**36.48%**			**9.13%**			**4.98%**			**1.13%**			**-0.68%**		

to the introduction of the EA, the population evolution process in our framework makes it unable to provide solutions right away (it generally takes several minutes). However, concerning the optimization ability, EA-DRL performs better than the AM on most test instances and obtains relatively small gaps w.r.t. the Gurobi results. The average gaps among all test instances produced by these compared approaches are obvious, as shown at the bottom of TABLE IV: while the accuracy of the solutions from the GA and GS is unsatisfactory and the average gap of the AM is 4.98%, the average gap of EA-DRL is only 1.13% with respect to Gurobi. In detail, we find that the AM has obvious advantages on a few instances, such as OP30 with a capacity of 3, OP50 with a capacity of 3 and OP80 with a capacity of 4, which are close to its training instances. Understandably, a model perform betters when the problem scales during training and testing are similar. However, our EA-DRL is particularly better than the AM on large-scale instances, such as OP150 and OP200, which reflects the better generalization ability of our framework.

Furthermore, we introduce the method of fine-tuning into our model to retrain it and improve its evaluation ability in specific instances. For a specific test instance, we can obtain an estimated number of nodes $\lfloor 1.3 * G \rfloor$ that may need to be planned according to greedy initialization. By randomly sampling $\lfloor 1.3 * G \rfloor$ nodes from the test instance repeatedly and eventually generating 5% of the regular training instances, a small-scale instance set can be used to retrain the model. Taking test instance OP80 with a capacity of 5 as an example, the retraining process of DYPN20 is shown in Fig. 7. While the process of fine-tuning is time-consuming, it can significantly improve the evaluation ability of the model. As shown in TABLE IV, the fine-tuned model (EA-DRL-FT) outperforms the other algorithms and obtains excellent solutions for these test instances. In approximately half of the test instances, EA-DRL-FT performs even better than Gurobi when running for 300 seconds and can also obtain solutions close to those of Gurobi in the remaining test instances. The average solution gap of EA-DRL-FT is -0.68%, which means that it can generate solutions that are slightly better than those of Gurobi.

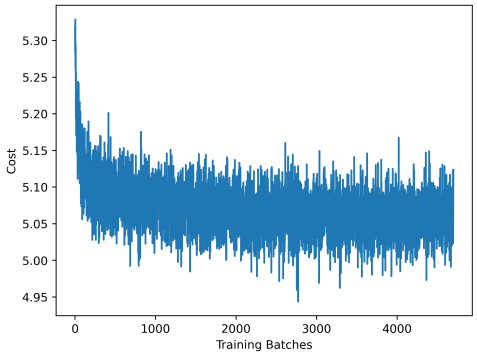

Fig. 7. Retraining process of DYPN20 for 4700 batches in test instance OP80 with a capacity of 5.

Note that since our models are trained on limited small-scale datasets but applied in unseen test instances with different node locations and dimensions, it is reasonable to find slight performance gaps between our approach and the state-of-the-art heuristic solver (Gurobi). On the other hand, we are not aiming to defeat the specialized, carefully designed linear programming solver that is Gurobi but are rather aiming to demonstrate the possibility of solving an OP by decomposing it into two subproblems and utilizing a framework combining EAs and DRL methods to replace pure EA or DRL models. The provision of such a new idea may provide researchers with more inspiration in their research concerning problems such as OPs and their variants.

C. Generalizability Validation

In this part, the generalization ability of the proposed model is analyzed in different OP instances. Since the composition of an OP includes the number of nodes as well as their locations, the capacity limitation and the node score distribution, we can consider the generalization ability of the model in terms of two aspects: the problem scale and node score distribution.

1) Generalization to Different Problem Scales: Regarding the generalization ability of the model for diverse problem scales, we have already evaluated its performance on instances with different capacity limitations, including OP20, OP30, OP50, OP80, OP100, OP150 and OP200, while our DRL models are only trained on the Node20, Node50 and Node100 instances. The evaluation results are listed in TABLE IV. As we can see, while our EA-DRL framework does perform slightly worse in test instances whose scales are very different from those of the training instances, such as OP150 and OP200, the gaps with respect to Gurobi are still small. Compared with that of our approach, the generalization performance of the AM is much poorer. This is understandable, as our deep learning module (DYPN) is designed for the TSP, while the AM is designed for the OP; an additional parameter, the capacity limitation, is required in the training stage of the AM, which makes it more difficult to adapt to problem scale changes. The experimental results confirm that the decomposition of the OP provides our framework with strong generalization ability.

2) Generalization to Different Node Score Distributions: Since the DYPN is in charge of planning the path and pays no attention to the node score distribution, our framework can achieve the same effect on all kinds of node score distributions in theory. In contrast, the performance of the AM may be somewhat affected by the node score distribution. To validate this idea, we regenerate test instances with the same problem scales (as listed in TABLE I) and the same location distribution (uniform distribution) but with a different node score distribution. We set the score of each node except the depot as a constant (i.e., 1) in the new instances and compare our method with the AM trained on instances with uniform node scores and Gurobi. The evaluation results are shown in TABLE V. While the average gap between the AM and Gurobi is small, the main contribution comes from OP100, and the AM performs poorly in most test instances. This also shows that the performance of Gurobi may be unstable due to minor changes in the problem. In contrast, EA-DRL performs well in most cases and sometimes even outperforms Gurobi. Compared with the evaluation results obtained on instances with uniform node scores (shown in TABLE IV), EA-DRL exhibits great generalization ability, which confirms our previous conjecture that node score distribution changes have little impact on our framework.

TABLE V
EVALUATION RESULTS OBTAINED WITH CONSTANT NODE SCORES

Node	Capacity	Gurobi (300 s)	AM(unif)		EA-DRL	
		score	score	gap	score	gap
20	2	11	10.00	9.09%	11.00	**0.00%**
	3	16	15.00	6.25%	16.00	**0.00%**
	4	18	16.00	11.11%	18.00	**0.00%**
30	2	16	15.00	6.25%	16.00	**0.00%**
	3	23	20.00	13.04%	23.00	**0.00%**
	4	27	24.00	11.11%	26.00	**3.70%**
50	3	31	29.00	6.45%	29.00	**6.45%**
	4	37	36.00	2.70%	36.20	**2.16%**
	5	45	41.00	8.89%	45.00	**0.00%**
80	4	48	48.00	**0.00%**	43.00	10.42%
	5	57	55.00	3.51%	56.00	**1.75%**
	6	68	62.00	8.82%	67.20	**1.18%**
100	5	55	64.00	**-16.36%**	62.40	-13.45%
	6	43	70.00	-62.79%	73.20	**-70.23%**
	7	57	77.00	-35.09%	85.80	**-50.53%**
150	8	120	109.00	9.17%	121.00	**-0.83%**
	9	132	118.00	10.61%	133.00	**-0.76%**
	10	145	125.00	13.79%	142.60	**1.66%**
200	9	162	150.00	7.41%	152.60	**5.80%**
	10	177	163.00	7.91%	169.20	**4.41%**
	11	190	165.00	13.16%	184.60	**2.84%**
AVG GAP		**0.00%**	**1.67%**		**-4.54%**	

VI. CONCLUSION

As some of the most classic combinatorial optimization problems, OPs widely arise in practical applications, such as tourist trip designs. However, as the problem scale grows in real-world applications, traditional methods are displaying shortcomings regarding their accuracies or solving speeds. Moreover, as the data in real-world cases always change dynamically, strong generalization ability is also required for constructed models. In this context, we creatively introduce a new OP solution framework in this study. We decompose an OP into a KP and a TSP and then introduce an EA as the KP solver and a deep learning approach as the TSP solver. Specifically, we improve NSGA-II and propose the DPCA, which maintains feasible and infeasible populations simultaneously to handle strong KP constraints. As the TSP solver, the DYPN is used to directly output a permutation of the input nodes and is trained by the REINFORCE algorithm. As an end-to-end approach, the DYPN can provide solutions immediately, thereby greatly reducing the complexity of solving the given OP. This framework shows satisfactory accuracy as well as great ability to generalize to unseen instances. While slight optimality gaps between our framework and the carefully designed Gurobi solver remain, our approach outperforms the GA and the state-of-the-art deep learning method AM in terms of both accuracy and generalization.

The proposed framework provides a new idea for solving OPs via the DM. In addition to its training difficulty, generalization and solution quality advantages, our framework has more potential on complex OPs such as multiobjective OPs and multimodal OPs, due to the advantages of EAs regarding these aspects. While our framework displays effectiveness in terms of solution quality, it is currently more suitable for large-scale dynamic problems that have low demand on solving time. How to obtain high-quality solutions in a short time period is still an urgent research objective for the future.

REFERENCES

[1] B. L. Golden, L. Levy, and R. Vohra, "The orienteering problem," *Naval Research Logistics (NRL)*, vol. 34, no. 3, pp. 307–318, 1987.

[2] P. Vansteenwegen, W. Souffriau, G. V. Berghe, and D. Van Oudheusden, "Iterated local search for the team orienteering problem with time windows," *Computers & Operations Research*, vol. 36, no. 12, pp. 3281–3290, 2009.

[3] P. Vansteenwegen, W. Souffriau, and D. Van Oudheusden, "The orienteering problem: A survey," *European Journal of Operational Research*, vol. 209, no. 1, pp. 1–10, 2011.

[4] G. Laporte and S. Martello, "The selective travelling salesman problem," *Discrete applied mathematics*, vol. 26, no. 2-3, pp. 193–207, 1990.

[5] R. Ramesh, Y.-S. Yoon, and M. H. Karwan, "An optimal algorithm for the orienteering tour problem," *ORSA Journal on Computing*, vol. 4, no. 2, pp. 155–165, 1992.

[6] A. C. Leifer and M. B. Rosenwein, "Strong linear programming relaxations for the orienteering problem," *European Journal of Operational Research*, vol. 73, no. 3, pp. 517–523, 1994.

[7] M. Fischetti, J. J. S. Gonzalez, and P. Toth, "Solving the orienteering problem through branch-and-cut," *INFORMS Journal on Computing*, vol. 10, no. 2, pp. 133–148, 1998.

[8] M. Gendreau, G. Laporte, and F. Semet, "A branch-and-cut algorithm for the undirected selective traveling salesman problem," *Networks: An International Journal*, vol. 32, no. 4, pp. 263–273, 1998.

[9] A. Gunawan, H. C. Lau, P. Vansteenwegen, and K. Lu, "Well-tuned algorithms for the team orienteering problem with time windows," *Journal of the Operational Research Society*, vol. 68, no. 8, pp. 861–876, 2017.

[10] V. Schmid and J. F. Ehmke, "An effective large neighborhood search for the team orienteering problem with time windows," in *International Conference on Computational Logistics*. Springer, 2017, pp. 3–18.

[11] Y. Amarouche, R. N. Guibadj, E. Chaalal, and A. Moukrim, "Effective neighborhood search with optimal splitting and adaptive memory for the team orienteering problem with time windows," *Computers & Operations Research*, vol. 123, p. 105039, 2020.

[12] C. Verbeeck, K. Sörensen, E.-H. Aghezzaf, and P. Vansteenwegen, "A fast solution method for the time-dependent orienteering problem," *European Journal of Operational Research*, vol. 236, no. 2, pp. 419–432, 2014.

[13] X. Chou, L. M. Gambardella, and R. Montemanni, "A tabu search algorithm for the probabilistic orienteering problem," *Computers & Operations Research*, vol. 126, p. 105107, 2021.

[14] A. Gunawan, H. C. Lau, and P. Vansteenwegen, "Orienteering problem: A survey of recent variants, solution approaches and applications," *European Journal of Operational Research*, vol. 255, no. 2, pp. 315–332, 2016.

[15] R. Gama and H. L. Fernandes, "A reinforcement learning approach to the orienteering problem with time windows," *Computers & Operations Research*, vol. 133, p. 105357, 2021.

[16] W. Kool, H. Van Hoof, and M. Welling, "Attention, learn to solve routing problems!" *arXiv preprint arXiv:1803.08475*, 2018.

[17] O. Vinyals, M. Fortunato, and N. Jaitly, "Pointer networks," *arXiv preprint arXiv:1506.03134*, 2015.

[18] I. Bello, H. Pham, Q. V. Le, M. Norouzi, and S. Bengio, "Neural combinatorial optimization with reinforcement learning," *arXiv preprint arXiv:1611.09940*, 2016.

[19] M. Nazari, A. Oroojlooy, L. V. Snyder, and M. Takáč, "Reinforcement learning for solving the vehicle routing problem," *arXiv preprint arXiv:1802.04240*, 2018.

[20] K. Li, T. Zhang, and R. Wang, "Deep reinforcement learning for multiobjective optimization," *IEEE transactions on cybernetics*, vol. 51, no. 6, pp. 3103–3114, 2020.

[21] M. Deudon, P. Cournut, A. Lacoste, Y. Adulyasak, and L.-M. Rousseau, "Learning heuristics for the tsp by policy gradient," in *International conference on the integration of constraint programming, artificial intelligence, and operations research*. Springer, 2018, pp. 170–181.

[22] J. K. Falkner and L. Schmidt-Thieme, "Learning to solve vehicle routing problems with time windows through joint attention," *arXiv preprint arXiv:2006.09100*, 2020.

[23] B. Lin, B. Ghaddar, and J. Nathwani, "Deep reinforcement learning for the electric vehicle routing problem with time windows," *IEEE Transactions on Intelligent Transportation Systems*, 2021.

[24] S. Gu and T. Hao, "A pointer network based deep learning algorithm for 0–1 knapsack problem," in *2018 Tenth International Conference on Advanced Computational Intelligence (ICACI)*. IEEE, 2018, pp. 473–477.

[25] S. Gu and Y. Yang, "A pointer network based deep learning algorithm for the max-cut problem," in *International Conference on Neural Information Processing*. Springer, 2018, pp. 238–248.

[26] L. Kai-Wen, Z. Tao, W. Rui, Q. Wei-Jian, H. Hui-Hui, and H. Hong, "Research reviews of combinatorial optimization methods based on deep reinforcement learning," *Acta Automatica Sinica*, vol. 47, no. 11, pp. 2521–2537, 2021.

[27] H. Dai, E. B. Khalil, Y. Zhang, B. Dilkina, and L. Song, "Learning combinatorial optimization algorithms over graphs," *arXiv preprint arXiv:1704.01665*, 2017.

[28] H. M. Salkin and C. A. De Kluyver, "The knapsack problem: a survey," *Naval Research Logistics Quarterly*, vol. 22, no. 1, pp. 127–144, 1975.

[29] R. Bellman, "Dynamic programming," *Science*, vol. 153, no. 3731, pp. 34–37, 1966.

[30] H. Kellerer, U. Pferschy, and D. Pisinger, "Multidimensional knapsack problems," in *Knapsack problems*. Springer, 2004, pp. 235–283.

[31] A. Bettinelli, V. Cacchiani, and E. Malaguti, "A branch-and-bound algorithm for the knapsack problem with conflict graph," *INFORMS Journal on Computing*, vol. 29, no. 3, pp. 457–473, 2017.

[32] T. K. Truong, K. Li, and Y. Xu, "Chemical reaction optimization with greedy strategy for the 0–1 knapsack problem," *Applied soft computing*, vol. 13, no. 4, pp. 1774–1780, 2013.

[33] K. Sörensen and M. Sevaux, "Ma— pm: memetic algorithms with population management," *Computers & operations research*, vol. 33, no. 5, pp. 1214–1225, 2006.

[34] B. A. Julstrom, "Greedy, genetic, and greedy genetic algorithms for the quadratic knapsack problem," in *Proceedings of the 7th annual conference on Genetic and evolutionary computation*, 2005, pp. 607–614.

[35] C. Changdar, G. Mahapatra, and R. K. Pal, "An improved genetic algorithm based approach to solve constrained knapsack problem in fuzzy environment," *Expert Systems with Applications*, vol. 42, no. 4, pp. 2276–2286, 2015.

[36] A. Homaifar, C. X. Qi, and S. H. Lai, "Constrained optimization via genetic algorithms," *Simulation*, vol. 62, no. 4, pp. 242–253, 1994.

[37] X. Hu, R. Eberhart *et al.*, "Solving constrained nonlinear optimization problems with particle swarm optimization," in *Proceedings of the sixth world multiconference on systemics, cybernetics and informatics*, vol. 5. Citeseer, 2002, pp. 203–206.

[38] G. Venter and J. Sobieszczanski-Sobieski, "Particle swarm optimization," *AIAA journal*, vol. 41, no. 8, pp. 1583–1589, 2003.

[39] K. E. Parsopoulos, M. N. Vrahatis *et al.*, "Particle swarm optimization method for constrained optimization problems," *Intelligent Technologies–Theory and Application: New Trends in Intelligent Technologies*, vol. 76, no. 1, pp. 214–220, 2002.

[40] T. P. Runarsson and X. Yao, "Stochastic ranking for constrained evolutionary optimization," *IEEE Transactions on evolutionary computation*, vol. 4, no. 3, pp. 284–294, 2000.

[41] T. Takahama and S. Sakai, "Constrained optimization by the ε constrained differential evolution with an archive and gradient-based mutation," in *IEEE congress on evolutionary computation*. IEEE, 2010, pp. 1–9.

[42] K. Deb, "An efficient constraint handling method for genetic algorithms," *Computer methods in applied mechanics and engineering*, vol. 186, no. 2-4, pp. 311–338, 2000.

[43] K. Deb, A. Pratap, S. Agarwal, and T. Meyarivan, "A fast and elitist multiobjective genetic algorithm: Nsga-ii," *IEEE transactions on evolutionary computation*, vol. 6, no. 2, pp. 182–197, 2002.

[44] K. Li, T. Zhang, R. W. Y. Wang, and Y. Han, "Deep reinforcement learning for combinatorial optimization: Covering salesman problems," *arXiv preprint arXiv:2102.05875*, 2021.

[45] K. Cho, B. Van Merriënboer, C. Gulcehre, D. Bahdanau, F. Bougares, H. Schwenk, and Y. Bengio, "Learning phrase representations using rnn encoder-decoder for statistical machine translation," *arXiv preprint arXiv:1406.1078*, 2014.

[46] R. J. Williams, "Simple statistical gradient-following algorithms for connectionist reinforcement learning," *Machine learning*, vol. 8, no. 3, pp. 229–256, 1992.

[47] D. P. Kingma and J. Ba, "Adam: A method for stochastic optimization," *arXiv preprint arXiv:1412.6980*, 2014.

[48] I. G. Optimization *et al.*, "Gurobi optimizer reference manual, 2018," *URL http://www. gurobi. com*, 2018.